

# <sup>1</sup>H/<sup>15</sup>N HSQC NMR Studies of Ligand Carboxylate Group Interactions with Arginine Residues in Complexes of Brodimoprim Analogues and *Lactobacillus casei* Dihydrofolate Reductase<sup>†,‡</sup>

William D. Morgan, Berry Birdsall, Pedro M. Nieto, Angelo R. Gargaro, and James Feeney\*

Molecular Structure Division, National Institute for Medical Research, The Ridgeway, Mill Hill, London NW7 1AA, U.K.

Received October 1, 1998; Revised Manuscript Received November 20, 1998

**ABSTRACT:** <sup>1</sup>H and <sup>15</sup>N NMR studies have been undertaken on complexes of *Lactobacillus casei* dihydrofolate reductase (DHFR) formed with analogues of the antibacterial drug brodimoprim (2,4-diamino-5-(3',5'-dimethoxy-4'-bromobenzyl)pyrimidine) in order to monitor interactions between carboxylate groups on the ligands and basic residues in the protein. These analogues had been designed by computer modeling with carboxylated alkyl chains introduced at the 3'-O position in order to improve their binding properties by making additional interactions with basic groups in the protein. Specific interactions between ligand carboxylate groups and the conserved Arg57 residue have been detected in studies of <sup>1</sup>H/<sup>15</sup>N HSQC spectra of complexes of DHFR with both the 4-carboxylate and the 4,6-dicarboxylate brodimoprim analogues. The spectra from both complexes showed four resolved signals for the four NH<sup>γ</sup> protons of the guanidino group of Arg57, and this is consistent with hindered rotation in the guanidino group resulting from interactions with the 4-carboxylate group in each analogue. In the spectra of each complex, one of the protons from each of the two NH<sub>2</sub> groups and both nitrogens are considerably deshielded compared to the shielding values normally observed for such nuclei. This pattern of deshielding is that expected for a symmetrical end-on interaction of the carboxylate oxygens with the NH<sup>γ12</sup> and NH<sup>γ22</sup> guanidino protons. The differences in the degree of deshielding between the complexes of the two structurally similar brodimoprim analogues and the methotrexate indicates that the shielding is very sensitive to geometry, most probably to hydrogen bond lengths. The <sup>1</sup>H/<sup>15</sup>N HSQC spectrum of the DHFR complex with the brodimoprim-6-carboxylate analogue does not feature any deshielded Arg NH<sup>γ</sup> protons and this argues against a similar interaction with the Arg57 in this case. It has not proved possible to determine whether the 6-carboxylate in this analogue is interacting directly with any residue in the protein. <sup>1</sup>H/<sup>15</sup>N HSQC spectra have been fully assigned for the complexes with the three brodimoprim analogues and chemical shift mapping used to explore interactions in the binding site. The <sup>1</sup>H signals of the bound ligands for all three brodimoprim analogues have been assigned. Their <sup>1</sup>H chemical shifts were found to be fairly similar in the different complexes indicating that the 2,4-diaminopyrimidine and the benzyl ring are binding in essentially the same binding sites and with the same overall conformation in the different complexes. The rotation rate about the N<sup>ε</sup>C<sup>δ</sup> bond in the brodimoprim-4,6-dicarboxylate complex with DHFR has been determined from a zz-HSQC exchange experiment, and its value is quite similar to that observed in the DHFR·methotrexate complex (24 ± 10 s<sup>-1</sup> at 8 °C and 50 ± 10 s<sup>-1</sup> at 15 °C, respectively). The <sup>1</sup>H and <sup>15</sup>N chemical shift differences of selected amide and guanidino NH groups, measured between the DHFR complexes, provided further evidence about the interactions involving Arg57 with the 4-carboxylate and 4,6-dicarboxylate brodimoprim analogues.

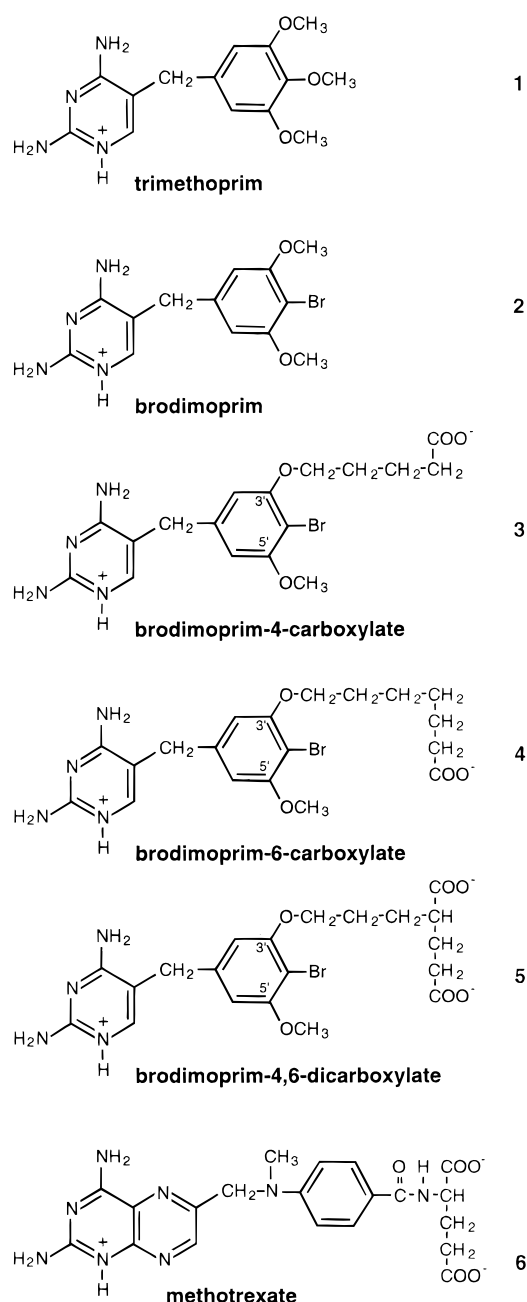
Dihydrofolate reductase catalyses the reduction of dihydrofolate to tetrahydrofolate using NADPH as a coenzyme. This enzyme is essential for cellular growth, and it has proved a useful target for antifolate drugs that act by inhibiting the enzyme in malignant and parasitic cells. One of these, trimethoprim (2,4-diamino-5-(3',4',5'-trimethoxybenzyl)pyrimidine) (**1**) is a clinically useful antibacterial drug which selectively inhibits dihydrofolate reductase in bacterial cells

(**1**). Many analogues of trimethoprim have been synthesized in attempts to find inhibitors which might have potential as improved antifolate drugs (2, 3). In previous studies, we examined a series of analogues of the related antibacterial drug brodimoprim (2,4-diamino-5-(3',5'-dimethoxy-4'-bromobenzyl)pyrimidine) (**2**) which had substituents at the 3'-O position designed to make additional interactions with basic groups in the protein (structures **3**–**5**; see Chart 1) (4). One of these analogues (**5**) has a 4,6-dicarboxylic acid side chain designed to interact with Arg57 and His28 in *Lactobacillus casei* dihydrofolate reductase, and this was found to bind a factor of 10<sup>3</sup> more tightly to the enzyme than did the parent molecule, brodimoprim (analogues **3** and **4** also bind 50 and 20 times more tightly as estimated from their respective K<sub>i</sub>

<sup>†</sup> This work was supported by funds from the Medical Research Council. PMN was funded by the Spanish Ministry of Education and Science.

<sup>‡</sup> The coordinates of the structure of the complex of *L. casei* DHFR and 4,6-dicarboxylate brodimoprim (**9**) have been deposited as PDB entries 1dis and 1diu.

Chart 1



values). Although analogue **5** retains its high specificity for the bacterial enzyme it did not prove to be an effective antibacterial agent due to reduced membrane permeability (5). Early NMR studies, based on considerations of <sup>1</sup>H chemical shifts, were used to determine the bound conformations of the ligand and also to monitor its specific interactions with His28 (4). The overall conformation of the two rings in the bound analogue appeared to be similar in the enzyme complexes formed with trimethoprim, brodimoprim, or the brodimoprim-4,6-dicarboxylate analogue. In the complex with the 4,6-dicarboxylate analogue, the pK<sub>a</sub> of His28 was increased by one unit compared to its value in the free enzyme (from 6.8 to 7.8). A similar increase had been detected earlier in NMR studies of complexes formed with substrate analogues containing glutamic acid moieties such as methotrexate **6** (6, 7). In the crystal structure of the methotrexate-NADPH-DHFR<sup>1</sup> complex (8), the γ-carboxylate group of the methotrexate glutamyl fragment is very

close to the imidazole ring of His28 and the change in pK<sub>a</sub> was interpreted as reflecting an ion–ion electrostatic interaction between the two groups. The similar increase in pK<sub>a</sub> of His28 was detected on forming the complex with the brodimoprim-4,6-dicarboxylate analogue **5** indicating that one of the carboxylate groups is interacting with His28 in a manner similar to that observed in the *L. casei* dihydrofolate reductase complex with methotrexate. In a subsequent <sup>1</sup>H NMR study of the complex of the brodimoprim-4,6-dicarboxylate analogue and *L. casei* dihydrofolate reductase (9) the intermolecular and intramolecular proton–proton NOEs were measured between protons on the ligand and the protein and used to provide distance constraints for inclusion in simulated annealing and energy minimization calculations to dock the brodimoprim-4,6-dicarboxylate into its binding site in the enzyme. This approach allowed the conformations of the aromatic rings to be determined (torsion angles  $\tau_1 = -153 \pm 4^\circ$  (C4–C5–C7–C1');  $\tau_2 = 53 \pm 4^\circ$  (C5–C7–C1'–C2')) and their binding sites to be defined. However, these studies were unable to define the interactions of the ligand carboxylate groups with specific groups on the enzyme.

Recently it has been shown that <sup>1</sup>H/<sup>15</sup>N HSQC NMR experiments can provide an effective method for characterizing interactions involving arginine guanidino groups with charged groups on ligands (10–15). The success of such studies relies on the relative ease of detection of <sup>1</sup>H and <sup>15</sup>N NMR signals from NH groups in <sup>15</sup>N-labeled proteins using gradient-enhanced two-dimensional <sup>1</sup>H/<sup>15</sup>N HSQC NMR experiments. The method has proved particularly useful for detecting the guanidino NH<sup>ε</sup> and NH<sup>η</sup> nuclei in arginine residues (see Figures 1 and 2). For example, in complexes of SH2 domains formed with bound phosphopeptides, several important arginine–ligand interactions between arginine NH<sup>η</sup> hydrogens and the phosphorylated tyrosines have been characterized (11–13). Similar interactions in complexes of *L. casei* dihydrofolate reductase between the guanidino group of the conserved Arg57 residue and a carboxylate group on the antifolate drug methotrexate (see Figure 1C) have also been detected (14). Our previous studies identified the arginine guanidino NH<sup>η</sup> hydrogens specifically involved in the interactions and characterized the structures and dynamics of the interacting groups (14, 15). Most of the arginine residues in proteins show only a single broad coalesced resonance in their <sup>1</sup>H/<sup>15</sup>N HSQC spectrum corresponding to the four NH<sup>η</sup> protons and two N<sup>η</sup> nitrogens in the guanidino group (see signals in the 73–79 ppm region in Figure 1). The coalesced signals arise from exchange between the NH<sup>η</sup> nuclei caused by rotations about the N<sup>ε</sup>C<sup>ε</sup> and C<sup>ε</sup>N<sup>η</sup> bonds. In a study of the complex of *L. casei* dihydrofolate reductase with methotrexate, four separate NH<sup>η</sup> signals were observed

<sup>1</sup> Abbreviations used: BDM, brodimoprim; BDM-4, brodimoprim-4-carboxylate; BDM-6, brodimoprim-6-carboxylate; BDM-4, 6, brodimoprim-4,6-dicarboxylate; COSY, correlated spectroscopy; DHFR, dihydrofolate reductase; DSS, sodium 2,2-dimethyl-2-silapentane-5-sulfonate; DQF, double quantum filtered;  $\Delta_{\text{TMP}}$ , chemical shift difference (ppm) between signal in specified DHFR complex and in the trimethoprim·DHFR complex; GARP, a broad-band decoupling sequence; HSQC, heteronuclear single quantum coherence spectroscopy; MTX, methotrexate; NMR, nuclear magnetic resonance; NOE, nuclear Overhauser effect; NOESY, nuclear Overhauser effect spectroscopy; PDB, Protein Data Bank; TMP, trimethoprim; TOCSY, total correlation time spectroscopy; 3D, three-dimensional; 2D, two-dimensional; 2D zz-HSQC, zz-magnetization exchange HSQC spectroscopy.

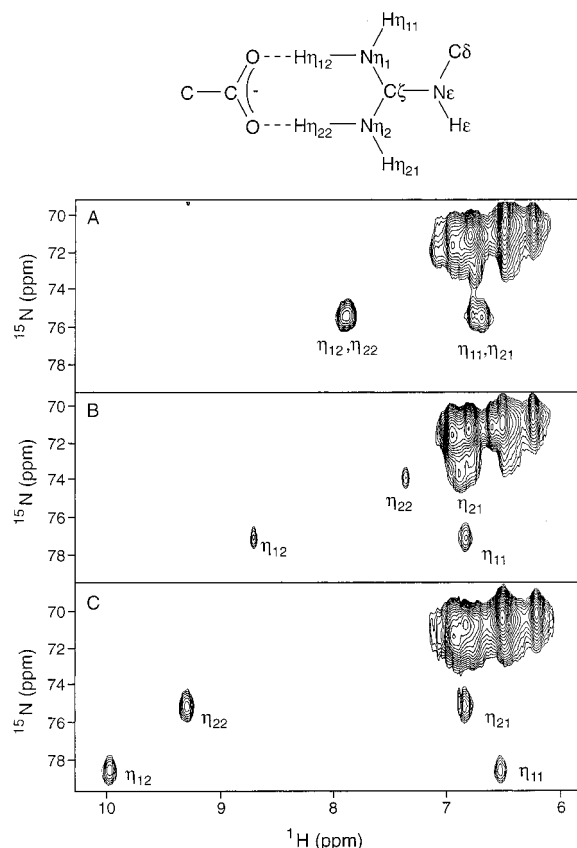


FIGURE 1: Expansion of the arginine guanidino  $\text{NH}^\eta$  region of the  $^1\text{H}/^{15}\text{N}$  HSQC spectra recorded at 600 MHz and 8 °C of *L. casei* DHFR complexed with (A) brodimoprim-4-carboxylate, (B) brodimoprim-4,6-dicarboxylate, and (C) methotrexate. The structure of the proposed symmetrical end-on interaction of the Arg57 guanidino group and a ligand carboxylate group is also shown.

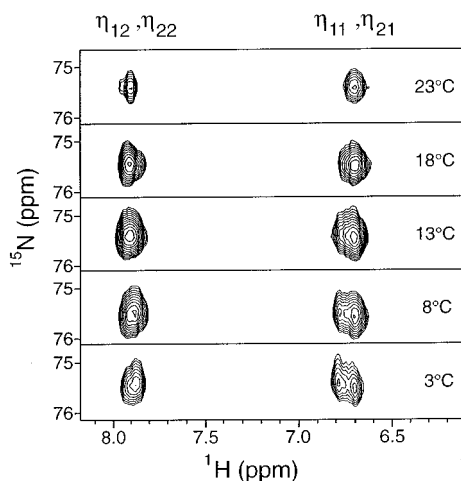


FIGURE 2: Regions of the  $^1\text{H}/^{15}\text{N}$  HSQC spectra showing the Arg57  $\text{NH}^\eta$  signals of *L. casei* DHFR complexed with brodimoprim-4-carboxylate (4 mM sample at 600 MHz) at a series of temperatures from 3 to 23 °C. The spectra at low temperatures (3 and 8 °C) clearly indicate that the  $\eta_{11}$  and  $\eta_{21}$  NH signals have different  $^1\text{H}$  and  $^{15}\text{N}$  frequencies.

for the Arg57 residue (Figure 1C) indicating hindered rotation in its guanidino group even at 20 °C (14). From a consideration of the  $^1\text{H}$  and  $^{15}\text{N}$  chemical shifts, it was possible to deduce that the Arg57 guanidino group interacts with the  $\alpha$ -carboxylate group of the glutamic acid moiety of methotrexate in an end-on symmetrical fashion (see structure in Figure 1) (8, 14). This information was incor-

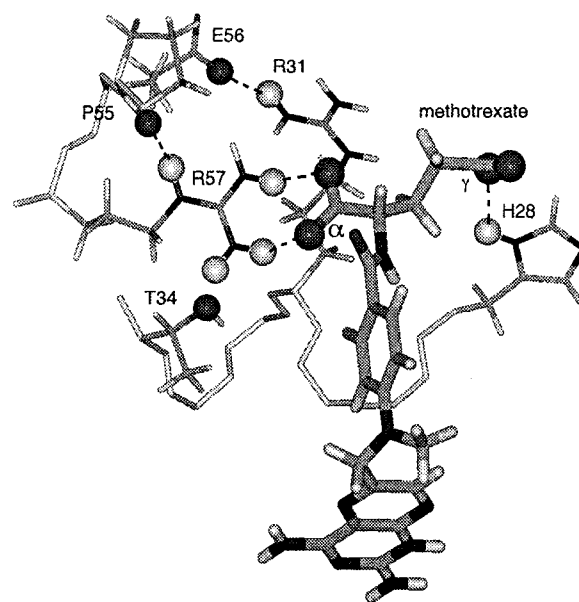


FIGURE 3: Part of the methotrexate binding site from the NMR-determined solution structure of the *L. casei* DHFR-methotrexate complex (16). The methotrexate  $\alpha$ -carboxylate group binds to Arg57 and its  $\gamma$ -carboxylate group binds to His28. (The  $\alpha$ - and  $\gamma$ -carboxylates of methotrexate correspond respectively to the 4- and 6-carboxylates of the brodimoprim-4,6-dicarboxylate analogue.) There are interactions linking Arg57 to Thr34 and Pro55, and the neighboring Glu56 backbone interacts with Arg31. The NH protons involved in these interactions are shown as light spheres, and the interacting oxygen atoms are as dark spheres.

porated into a solution structure determination of the *L. casei* DHFR-methotrexate complex and part of the methotrexate binding site from this structure determination is shown in Figure 3 (16). From observations of temperature-dependent line shape changes of the  $\text{NH}^\eta$  signals and from results of  $zz$ -HSQC exchange experiments, rates of rotations about the  $\text{N}^\epsilon\text{C}^\zeta$  and  $\text{C}^\zeta\text{N}^\eta$  bonds were determined and shown to indicate the presence of correlated rates of rotation about the Arg57  $\text{N}^\epsilon\text{C}^\zeta$  bond and the methotrexate  $\text{C}\alpha\text{-C}'$  bond in its bound glutamyl moiety (15).

The aim of the present work is carry out similar experiments on DHFR complexes with the brodimoprim analogues (3–5) in order to monitor interactions between carboxylate groups on the ligands and basic residues in the protein by measuring  $^1\text{H}$  and  $^{15}\text{N}$  chemical shift perturbations for protein NH signals, mainly those from arginine residues.

## MATERIALS AND METHODS

$^{15}\text{N}$ -labeled *L. casei* DHFR was expressed in *Escherichia coli* cells grown on a minimal medium and isolated and purified as described previously (17, 18). The brodimoprim analogues 3–5 were kindly provided by Dr I. Kompis, Hoffman-La-Roche (4). All other chemicals used were of analytical grade.

The NMR experiments were performed on equimolar complexes of DHFR formed with analogues 3–5 examined as 0.6 mL samples (1 or 4 mM) in 90%  $\text{H}_2\text{O}/10\%$   $\text{D}_2\text{O}$  and 50 mM potassium phosphate and 100 mM KCl,  $\text{pH}^*$  6.5 (the  $\text{pH}^*$  values are meter readings, unadjusted for deuterium isotope effects).

The NMR experiments were performed at 3–40 °C on Varian 500 and 600 MHz spectrometers. All of the NMR



experiments used the Watergate technique for water suppression (19) and the GARP sequence (20) for  $^{15}\text{N}$  decoupling during the detection period. Quadrature detection in all indirectly detected dimensions was achieved using the method of States and co-workers (21).

The 2D  $^1\text{H}/^{15}\text{N}$  HSQC sequence used in the experiments was essentially the same as that proposed by Mori and co-workers (22). These experiments were performed using the following parameters for the  $^1\text{H}$  and  $^{15}\text{N}$  dimensions respectively: sweep widths 8000 Hz ( $^1\text{H}$ ) and 4000 Hz ( $^{15}\text{N}$ ); 2432 data points ( $^1\text{H}$ ) and 180  $t_1$  increments ( $^{15}\text{N}$ ); processed after zero-filling to 4K ( $^1\text{H}$ ) and 1K data points ( $^{15}\text{N}$ ). The 2D zz-HSQC experiments (23, 24) used for the exchange studies were carried out at 8 °C using a pulse sequence described by Yamazaki and co-workers (12). The experiment has a modified gradient enhanced HSQC pulse sequence in which a mixing time is inserted just prior to the transfer of magnetization from  $^{15}\text{N}$  to  $^1\text{H}$ . This allows observation of the transference of  $^{15}\text{N}$ -labeled heteronuclear zz-magnetization ( $I_zS_z$ ) between the different sites. The experiment was carried out with a series of different mixing times (2, 6, 12, 18, and 24 ms). The data were processed with zero-filling in both dimensions using Varian software (VNMR, version 5.1).

The rate constants were obtained from the zz-HSQC exchange experiments by measuring the normalized intensities of the cross-peak,  $I = [\text{cross-peak volume}/(\text{cross-peak} + \text{autopeak}) \text{ volumes}]$  at different mixing times and analyzing the data using a nonlinear regression analysis. Assuming a two-site exchange and neglecting cross relaxation during the mixing time, the normalized cross-peak intensity as a function of the mixing time ( $\tau_m$ ) is given by the expression  $I(\tau_m) = 0.5[1 + \exp(-2k\tau_m)]$ , where  $k$  is the rate constant of the exchange process (23).

Rate constants were also determined from line shape analysis using the standard equations for exchange processes (15, 25).

## RESULTS AND DISCUSSION

To explore the specific protein–ligand interactions involving arginine residues we have examined the  $^1\text{H}/^{15}\text{N}$  HSQC spectra for the binary complexes of *L. casei* DHFR with the three brodimoprim analogues **3–5** (brodimoprim-4-carboxylate, 6-carboxylate, and 4,6-dicarboxylate, respectively). The HSQC spectral region of most interest contains signals from the guanidino group  $\text{NH}^\eta$  nuclei of the 8 arginine residues in the protein (see Figure 1). The  $^1\text{H}$  and  $^{15}\text{N}$  resonance assignments for the  $\text{NH}^\eta$  signals in arginine residues in the DHFR•methotrexate and DHFR•methotrexate•NADPH complexes were made earlier by using 3D  $^1\text{H}/^{15}\text{N}$  HSQC-TOCSY and HSQC–NOESY experiments (14, 15). Similar methods were used here to make the assignments for the complexes with the brodimoprim analogues **3–5**, and Table 1 summarizes the  $^1\text{H}$  and  $^{15}\text{N}$  chemical shifts for nuclei in the NH groups of arginine residues in DHFR and its complexes with methotrexate, trimethoprim, and the brodimoprim analogues **3–5**. In earlier work (14), it was shown that the only way in which a carboxylate group can interact with the  $\text{NH}^\eta$  protons of Arg57 to perturb the shielding of the two centrally situated  $\text{NH}^{\eta12}$  and  $\text{NH}^{\eta22}$  protons is for the carboxylate oxygen atoms to form hydrogen bonds with these centrally

Table 1:  $^1\text{H}$  and  $^{15}\text{N}$  Chemical Shifts for NH Groups in Arginine Residues in Complexes of *L. casei* DHFR<sup>a</sup>

residue	atom	BDM-6	BDM-4	BDM-4,6	MTX
Arg9	N <sup>ε</sup>	85.35	85.40	85.41	85.10
Arg9	H <sup>ε</sup>	7.28	7.27	7.27	7.33
Arg31	N <sup>ε</sup>	85.69	86.35	85.55	85.70
Arg31	H <sup>ε</sup>	7.44	7.52	7.52	7.39
Arg52	N <sup>ε</sup>	81.37	81.96	81.74	81.40
Arg52	H <sup>ε</sup>	6.58	6.81	6.78	6.69
Arg57	N <sup>ε</sup>	81.56	81.91	82.05	79.90
Arg57	H <sup>ε</sup>	5.84	5.85	5.99	5.66
Arg57	N <sup>η1</sup>		75.42	77.1	75.00
Arg57	H <sup>η11</sup>		6.70	6.83	6.89
Arg57	H <sup>η12</sup>		7.91	8.71	9.33
Arg57	N <sup>η2</sup>		75.33	73.84	79.00
Arg57	H <sup>η21</sup>		6.79	6.89	6.77
Arg57	H <sup>η22</sup>		7.87	7.36	10.17
Arg43	N <sup>ε</sup>	85.51	85.80	85.32	85.10
Arg43	H <sup>ε</sup>	8.40	8.43	8.34	8.32
Arg44	N <sup>ε</sup>	84.01	83.98	84.07	84.00
Arg44	H <sup>ε</sup>	7.19	7.19	7.21	7.29
Arg117	N <sup>ε</sup>	85.14	85.29	85.23	85.40
Arg117	H <sup>ε</sup>	8.33	8.34	8.33	8.52
Arg142	N <sup>ε</sup>	83.31	83.35	83.33	83.10
Arg142	H <sup>ε</sup>	7.41	7.41	7.40	7.44

<sup>a</sup>  $^1\text{H}$  shifts (errors  $\pm 0.02$  ppm) referenced to DSS and  $^{15}\text{N}$  shifts (errors  $\pm 0.07$  ppm) from liquid  $\text{NH}_3$  (see reference (14)).

situated hydrogens in a manner described as a type 1 interaction by Lancelot et al. (26) and shown in Figure 1. In an analysis of arginine–aspartate interactions found in X-ray structures of proteins by Mitchell et al. (27), such an end-on symmetric structure was found to be one of the most favored orientations for intermolecular interactions between arginine guanidino  $\text{NH}_2$  and carboxylate groups. This model is fully consistent with the large downfield shifts seen for the Arg57  $\text{NH}^{\eta12}$  (10.17 ppm) and  $\text{NH}^{\eta22}$  (9.33 ppm) signals seen for the DHFR•methotrexate complex (Figure 1C). Yamazaki et al. (11) reported similar results for a complex of the SH2 domain and a phosphotyrosyl peptide where they suggested that the hindered rotation resulted from the interactions between the arginine guanidino  $\text{NH}_2$  groups and a phosphate group. In this case, the  $\text{NH}^{\eta12}$  and  $\text{NH}^{\eta22}$  protons formed hydrogen bonds with the phosphate oxygen atoms.

The chemical shift data for the backbone NH groups for all residues in the protein and its complexes are provided in Table 1 of the Supporting Information. These assignments were also made using 3D  $^1\text{H}/^{15}\text{N}$  HSQC-TOCSY and HSQC–NOESY experiments. Table 2 of the Supporting Information shows a list of residues which have NH signals showing substantial differences in their  $^1\text{H}$  or  $^{15}\text{N}$  chemical shifts ( $\Delta_{\text{TMP}}$  values) between DHFR complexes with trimethoprim and those with the brodimoprim analogues. Chemical shift differences observed between signals from corresponding nuclei in different complexes will reflect binding differences between the different ligands.

Homocuclear 2D DQF COSY, TOCSY, and NOESY spectra were also recorded for the various complexes, and the  $^1\text{H}$  chemical shift assignments for the bound brodimoprim analogues **3–5** were made using methods described previously (see data in Table 2) (9, 28). The  $^1\text{H}$  chemical shifts of the bound ligands are fairly similar in the different complexes indicating that the 2,4-diaminopyrimidine and the benzyl ring are binding in essentially the same binding sites in the different complexes. The H6, H2', and H6' protons

Table 2:  $^1\text{H}$  Chemical Shifts (ppm<sup>a</sup>) of the Bound Ligands in Complexes of DHFR with Trimethoprim and Brodimoprim Analogues

atom	TMP <sup>b</sup>	BDM-4,6	BDM-4	BDM-6
H2'	5.86 <sup>c</sup> (4.97 <sup>d</sup> )	5.05	4.98	
H6'	5.86 <sup>c</sup> (6.81 <sup>d</sup> )	6.93	6.89	6.88
5'-OCH <sub>3</sub>	(3.83 <sup>d</sup> )	3.98	3.98	3.95
H7A	3.74	3.89	3.88	3.89
H7B	3.22	3.49	3.38	3.41
H6	6.52	6.51	6.60	6.64
NH1	14.85	14.99	15.24	14.97 <sup>e</sup>
HN2A	10.46	10.53	10.48	10.53
HN2B	5.90	5.90	5.96	6.08
HN4A	9.18	9.41		
HN4B	7.18	7.32		

<sup>a</sup> Referenced to DSS. <sup>b</sup> Martorell et al., (1994), ref (28). <sup>c</sup> Averaged signals at 35 °C. <sup>d</sup> Measured at 5 °C (unpublished results). <sup>e</sup> Measured at 8 °C.

are particularly sensitive to the overall conformation of the ligand and their similar values in the different complexes indicate that the bound ligands have similar values for their  $\tau_1$  and  $\tau_2$  torsion angles (29).

**DHFR•brodimoprim-4-carboxylate Complex.** The  $^1\text{H}/^{15}\text{N}$  HSQC spectrum of this complex recorded at 8 °C (Figure 1A) shows one set of arginine guanidino  $\text{NH}^\eta$  signals displaced downfield from the main group of  $\text{NH}^\eta$  signals. These signals were assigned to Arg57 on the basis of  $^1\text{H}/^{15}\text{N}$  HSQC-TOCSY and HSQC-NOESY experiments. It can be seen in Figure 2 that at low temperatures (3, 8, and 13 °C) four resolved signals are observed for the four  $\text{NH}^\eta$  protons. The downfield displacement of the Arg57 guanidino  $\text{NH}^\eta$   $^1\text{H}$  and  $^{15}\text{N}$  chemical shifts to give four resolved signals, indicates that the ligand is interacting with the arginine and causing hindered rotation in its guanidino group. The two lowest field signals 7.87 and 7.90 ppm at 3 °C are from protons attached to different  $\text{N}^\eta$  atoms, and their low-field  $^1\text{H}$  chemical shifts indicate that one proton from each  $\text{NH}_2$  group is hydrogen bonding to the ligand. This would suggest that there is a symmetrical end-on bidentate interaction of the Arg57 guanidino group with the 4-carboxylate group similar to that seen previously in the methotrexate•DHFR complex (see structure in Figure 1). The observed signals for the  $\text{NH}^{\eta_{12}}$  and  $\text{NH}^{\eta_{22}}$  protons have very similar chemical shifts, and this indicates that the interactions for each of the two  $\text{NH}_2$  groups in the complex are fairly similar. Thus the 4-carboxylate group is interacting with Arg57 in a manner similar to, but not identical with, that previously observed for the  $\alpha$ -carboxylate group of the glutamate moiety in methotrexate in its complex with DHFR.

In the low-temperature spectra (3–8 °C), the  $^1\text{H}$  chemical shift difference between the  $\eta_{11}$  and  $\eta_{21}$  signals is 48 Hz and line shape analysis indicates that the rate of rotation about the  $\text{N}^\epsilon\text{--C}^\zeta$  bond must be less than 60  $\text{s}^{-1}$  at 8 °C. As the temperature is raised from 3 to 28 °C, the signals show no indication of coalescing, but one pair of signals (at 6.79 and 7.88 ppm) progressively broadens such that at 28 °C only one pair signals (at 6.71 and 7.91 ppm) can be detected. The broadened signals arise from one of the  $\text{NH}_2$  groups, and the broadening is caused by the presence of a dynamic process which could involve either exchange between the  $\text{NH}^\eta$  protons resulting from rotation about one of the  $\text{C}^\zeta\text{--N}^\eta$  bonds or, less likely, exchange of the  $\text{NH}^\eta$  protons with

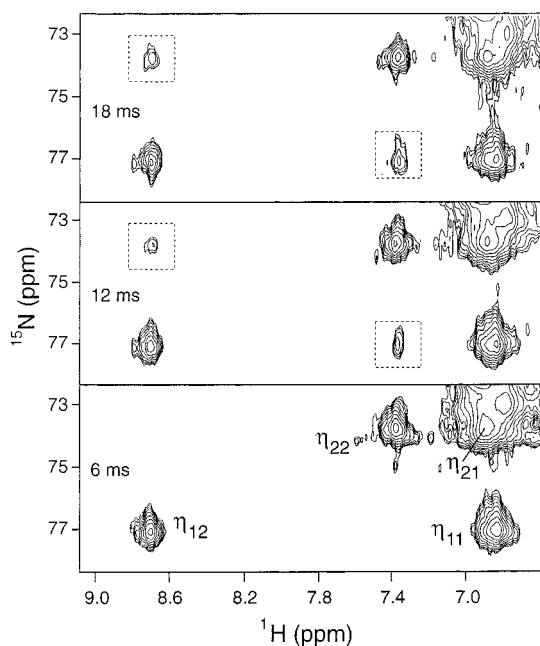


FIGURE 4: Parts of the zz-HSQC spectra recorded at 600 MHz showing the guanidino  $\text{NH}^\eta$  signals of Arg57 in the complex of *L. casei* dihydrofolate reductase with brodimoprim-4,6-dicarboxylate as a function of the mixing times (6, 12, and 18 ms). The exchange peaks are shown in boxes in the spectra.

the water protons. At lower temperatures (3 °C), line shape analysis of the pairs of  $\text{NH}_2$  signals indicates that the rates of rotation about the  $\text{C}^\zeta\text{--N}^\eta$  bonds are less than 200  $\text{s}^{-1}$ .

**DHFR•brodimoprim-6-dicarboxylate Complex.** The  $^1\text{H}/^{15}\text{N}$  HSQC spectrum of this complex (not shown) does not have any signals from an arginine guanidino group with chemical shifts different from the main group of signals: thus there is no indication that the 6-carboxylate analogue is interacting with the Arg57 guanidino group. It has not been possible to assign the protein residue or residues which bind to the 6-carboxylate group. However, from a consideration of the  $^1\text{H}$  and  $^{15}\text{N}$  chemical shift differences ( $\Delta_{\text{TMP}}$ ) between DHFR complexes with trimethoprim and with analogues 3–5, it can be confirmed that His28 is not involved in the interaction (see later). Previous work on the dihydrofolate reductase complex with the methotrexate  $\alpha$ -amide analogue where only the  $\gamma$ -carboxylate (equivalent to the 6-position in the brodimoprim analogue) is available for binding showed that there was no interaction of the  $\gamma$ -carboxylate group with His 28 (7). Similar behavior is seen in the complex with the brodimoprim-6-carboxylate analogue; when the interaction between the 4- (or  $\alpha$ -) carboxylate group and Arg 57 is absent, the interaction of the 6- (or  $\gamma$ -) carboxylate with His 28 is not formed.

**DHFR•brodimoprim-4,6-dicarboxylate Complex.** In the  $^1\text{H}/^{15}\text{N}$  HSQC spectrum of this complex (Figure 1B) one set of four guanidino  $\text{NH}^\eta$  signals are found displaced from the position of the main group of  $\text{NH}^\eta$  signals. Unequivocal evidence that these signals originate from the same guanidino group comes from the detection of autocorrelation peaks between these signals in zz-HSQC exchange experiments (see Figure 4). The signals were assigned to the  $\text{NH}^\eta$  nuclei in Arg57 using 3D  $^1\text{H}/^{15}\text{N}$  HSQC-NOESY and HSQC-TOCSY methods. The NOE connections between the  $\text{NH}^\epsilon$  proton and the  $\text{NH}^\eta$  protons allowed the assignment of the

$\eta_1$  and  $\eta_2$  NH protons. The observation of four signals clearly indicates the presence of hindered rotation in the guanidino group presumably caused by interactions with one of the carboxylate groups. Again, one signal from each of the NH<sub>2</sub> groups is deshielded which is consistent with an end-on interaction as shown in Figure 1. The group interacting with Arg57 has been assigned to the 4-carboxylate group which was found to interact with Arg57 in the earlier study of the DHFR complex with the brodimoprim-4-carboxylate analogue.

For the complex with the brodimoprim-4,6-dicarboxylate, it proved possible to measure the relatively slow rates of rotation about the N<sup>ε</sup>C<sup>ζ</sup> bond by using a zz-HSQC exchange experiment (12, 15, 23, 24). This experiment uses a modified gradient enhanced HSQC pulse sequence (12) to detect exchange processes involving NH groups as described earlier. Figure 4 shows the spectra from a zz-HSQC experiment on the DHFR complex formed with the 4,6-dicarboxylate analogue and carried out at 8 °C with a series of mixing times. Spectra recorded with decreasing mixing times showed a progressive decrease in intensity of the exchange peaks with decrease in mixing time. Cross-peak correlations are seen between peaks which are related to corresponding protons in the NH<sup>η</sup> group (NH<sup>η12</sup> with NH<sup>η22</sup>). These connections are due to rotations about the N<sup>ε</sup>C<sup>ζ</sup> bond which result in interchange of the positions of the two NH<sub>2</sub> groups. The rate constant can be obtained from analysis of the changes in cross-peak intensities as a function of mixing time as indicated in the Materials and Methods section and a value of  $24 \pm 10 \text{ s}^{-1}$  was determined for the N<sup>ε</sup>C<sup>ζ</sup> rotation at 8 °C. In an earlier study on the methotrexate complex (15), a rate constant for this rotation of  $50 \pm 10 \text{ s}^{-1}$  was determined at 15 °C. Thus these rates of rotation are quite similar in the two complexes. It was not possible to carry out the zz-HSQC experiment with the complex formed with the 4-carboxylate analogue because of the very small separation between the two <sup>15</sup>N signals.

**<sup>1</sup>H and <sup>15</sup>N Chemical Shift Differences between NH Groups in Different Complexes.** Some additional information relating to the presence or absence of specific interactions with His28 and Arg57 can be obtained by examining the differences in chemical shifts for NH groups in different complexes. For example, characteristic differences in <sup>1</sup>H/<sup>15</sup>N chemical shifts ( $\Delta_{\text{TMP}}$ ) observed for Thr34 and adjacent residues between the complexes with a 4-carboxylate containing analogue and with trimethoprim (see Table 2 of Supporting Information) provide information about the 4-carboxylate interaction with the Arg57 residue. It can be seen in Figure 3 that one of the NH<sup>η</sup> of Arg57 forms a hydrogen bond with the hydroxyl oxygen of Thr34: a consequence of this is that interactions between a ligand carboxylate group and the guanidino group of Arg57 can cause indirect changes in the NH chemical shifts of Thr34 and its adjacent residues, Val35, Gly36 and Lys37. For example, the signals from these residues show large differences in chemical shifts between the complexes with trimethoprim and methotrexate ( $\Delta_{\text{TMP}}$  <sup>15</sup>N and <sup>1</sup>H values for methotrexate are Thr34, 1.50 and 0.15 ppm; Val35, -0.75 and 0.47 ppm; Gly36, -0.75 and 0.0 ppm; Lys37, 0.55 and 0.17 ppm, respectively). It can be seen that signals from these residues also have large  $\Delta_{\text{TMP}}$  values in the case of the 4-carboxylate (Thr34, 1.03 and 0.12 ppm; Val35, -0.90 and 0.26 ppm; Gly36, -0.66 and 0.03 ppm; Lys37, 0.49 and

0.17 ppm, respectively, for <sup>15</sup>N and <sup>1</sup>H shift differences) and 4,6-dicarboxylate analogues (Thr34, 1.04 and 0.17 ppm; Val35, -2.08 and 0.29 ppm; Gly36, -0.91 and -0.02 ppm; Lys37, 0.38 and 0.12 ppm, respectively, for <sup>15</sup>N and <sup>1</sup>H shift differences) which both have interactions between a carboxylate group and Arg57. In contrast, only very small shift differences are observed for the 6-carboxylate analogue (Thr34, 0.22 and 0.00 ppm; Val35, 0.08 and 0.03 ppm; Gly36, 0.15 and -0.03 ppm; Lys37, 0.04 and -0.05 ppm, respectively, for <sup>15</sup>N and <sup>1</sup>H shift differences) confirming that it does not bind to Arg57.

Earlier work showed that neither the 4-carboxylate nor the 6-carboxylate analogue perturb the pK<sub>a</sub> of His28, and thus these analogues are not interacting electrostatically with this residue (4). However, the backbone NH chemical shift of His28 shows a significant shift differences  $\Delta_{\text{TMP}}$  for all three analogues 3–5 (see Table 2 of Supporting Information) because the alkyl substituent at the 3'-O position in all of the analogues is near to the backbone of His28. In the case of the complex with the 4,6-analogue, a very large chemical shift difference for the backbone NH of His28 was observed (an <sup>15</sup>N  $\Delta_{\text{TMP}}$  shift difference of -4.1 ppm, see Table 2 of Supporting Information), and this probably reflects the direct electrostatic interaction between one of its carboxylate groups and His28 which has previously been characterized (4).

There are chemical shift changes ( $\Delta_{\text{TMP}}$ ) noted for residues in the loop Phe49-Leu 54 for all three analogues (see Table 2 of Supporting Information), and these effects probably arise from the replacement of the trimethoprim 4'-OCH<sub>3</sub> group by a bromo substituent in analogues 3–5. For example, Phe49 is in close proximity to the 4'-bromo substituent (9) and its backbone carbonyl oxygen is within hydrogen-bonding distance of NH<sup>ε</sup> of Arg52. Clearly, small changes in the position of the bromo substituent in the complexes with analogues 3–5 could cause  $\Delta_{\text{TMP}}$  changes at Arg52.

A comparison of the  $\Delta_{\text{TMP}}$  values for the 6-carboxylate and 4,6-dicarboxylate analogue complexes for residues 25–28 confirms that the carboxylate group in complex with the 6-carboxylate is not forming an electrostatic interaction with His28. However, the data in Table 2 of Supporting Information are unable to provide an unequivocal assignment of the interacting residue in the DHFR•brodimoprim-6-carboxylate complex. Significant  $\Delta_{\text{TMP}}$  values are noted for Arg31, Arg52, and Arg57. Arg52 is too far away to be directly involved in binding to the carboxylate group, and the observed small changes for this residue could be due to differences in the position of the 4'-bromo substituent. If the interaction were with Arg57 it would need to be different from the interactions seen with the 4-carboxylate- and 4,6-dicarboxylate-containing analogues because of the low  $\Delta_{\text{TMP}}$  values for residues 34–37 and the nondetection of Arg57 NH<sup>η</sup> signals in the complex with the 6-carboxylate analogue. An interaction of the 6-carboxylate group with Arg31 seems the most likely, but one cannot exclude the possibility that it is binding to the side chain of Lys51.

## CONCLUSIONS

In earlier NMR and modeling studies of complexes of DHFR with the brodimoprim analogues 3–5, the NMR determined pK<sub>a</sub> value of His28 proved to be a useful probe



for determining whether it interacted with a ligand carboxylate group in the various complexes. For example, it was found that binding the brodimoprim 4,6-dicarboxylate analogue to DHFR caused an increase in the  $pK_a$  of His28 by one unit. This was as predicted because the 4,6-dicarboxylate side chain on the benzyl ring of brodimoprim had been designed to mimic the interactions of the glutamate moiety in methotrexate. In contrast, the 6-carboxylate analogues of brodimoprim did not perturb the  $pK_a$  value of His28 (nor that of any other histidine) in *L. casei* DHFR, although modeling studies indicate that such an interaction should be feasible. The  $pK_a$  of His28 also remained unperturbed in the complex with the 4-carboxylate analogue, but this was not surprising because modeling studies had predicted that the 4-carboxylate would mimic the  $\alpha$ -carboxylate of methotrexate and interact with Arg57 (4). The work reported here has allowed such interactions to be monitored directly. The 4-carboxylate and the 4,6-dicarboxylate brodimoprim analogues have both been shown to interact with Arg57 causing hindered rotation in its guanidino group and perturbing the NH  $^1H$  and  $^{15}N$  chemical shifts from their normal values. In each case both nitrogens and one of the protons from each of the two  $NH_2$  groups are considerably deshielded compared to the shielding values normally observed for such nuclei. This, together with the hindered rotation, provides evidence for a symmetrical end-on hydrogen-bonding interaction with a carboxylate group of the type deduced previously in the DHFR-methotrexate complex (see structure in Figure 1) (14, 15). The rotation rate about the  $N^{\epsilon}C^{\delta}$  bond in the 4,6-dicarboxylate complex with DHFR is quite similar to that observed in the DHFR-methotrexate complex ( $24 \pm 10 \text{ s}^{-1}$  at  $8^\circ\text{C}$  and  $50 \pm 10 \text{ s}^{-1}$  at  $15^\circ\text{C}$ , respectively).

The observed downfield shifts of the  $NH^{\eta}$  protons for the complexes with **3** and **5** (Figure 1B,C) are smaller than those observed in the DHFR-methotrexate complex. From consideration of correlations between  $^1H$  chemical shifts and hydrogen bond lengths reported from solid-state NMR studies of crystalline materials (30), the chemical shifts are known to be very sensitive to changes in hydrogen bond lengths. The measured  $^1H$  chemical shifts for the  $NH^{\eta12}$  and  $NH^{\eta22}$  protons for Arg57 in the DHFR-methotrexate complex correspond to hydrogen bond distances ( $O\cdots H-N$ ) of about 2.3–2.4 Å. The  $^1H$  shifts observed for 4-carboxylate complex would correspond to slightly longer hydrogen bonds (0.2 Å longer), and the same is true for the average shift in the 4,6-dicarboxylate complex. The observed  $^1H$  shifts of the  $NH^{\eta12}$  and  $NH^{\eta22}$  for the latter suggest that the interaction with the 4,6-dicarboxylate has a slightly more asymmetric arrangement of hydrogen bonds probably caused by its need to accommodate the interaction of its 6-carboxylate group with His28.

Detailed NMR structural studies on complexes of dihydrofolate reductase with methotrexate (16) (PDB; A108) and trimetrexate (31) (PDB; 1bzf) indicate that the side chain of Arg 57 is in essentially the same position in both complexes even though there is no possibility of an interaction between the arginine guanidino group and a ligand carboxylate group in the latter complex. It would appear that even in the absence of a benzoyl glutamate moiety, the Arg 57 side chain is already correctly positioned for its interaction with the  $\alpha$ -carboxylate group of methotrexate leading to no entropy

loss on binding and thus contributing to its high binding affinity. In the case of the complexes with the brodimoprim-4-carboxylate and -4,6-dicarboxylate analogues, it seems likely that the position of the Arg 57 side chain will be similar to that in the methotrexate complex and that the interactions with the 4-carboxylate groups result in formation of similar hydrogen bonds but with small differences in the hydrogen bond lengths.

## ACKNOWLEDGMENT

We thank J. E. McCormick for expert technical assistance and V. I. Polshakov for providing the line shape analysis program.

## SUPPORTING INFORMATION AVAILABLE

Tables of  $^1H$  and  $^{15}N$  chemical shift data. This material is available free of charge via the Internet at <http://pubs.acs.org>.

## REFERENCES

1. Blakley, R. L. (1985) *Dihydrofolate Reductase in Foliates and Pterins*. Blakley, R. L., and Benkovic, S. J., Eds., Vol. 1, Chapter 5, pp 191–253, J. Wiley, New York.
2. Roth, B., and Cheng, C. C. (1982) *Prog. Med. Chem.* 19, 1–58.
3. Kuyper, L. F., Roth, B., Baccanari, D. P., Ferone, R., Beddell, C. R., Champness, J. N., Stammers, D. K., Dann, J. G., Norrington, F. E. A., Baker, D. J., and Goodford, P. J. (1982) *J. Med. Chem.* 25, 1120–1122.
4. Birdsall, B., Feeney, J., Pascual, C., Roberts, G. C. K., Kompis, I., Then, R. L., Muller, K., and Kroehn, A. (1984) *J. Med. Chem.* 23, 1672–1676.
5. Kompis, I., and Then, R. L. (1984) *Eur. J. Med. Chem.* 19, 529–534.
6. Birdsall, B., Griffiths, D. V., Roberts, G. C. K., Feeney, J., and Burgen, A. S. V. (1977) *Proc. R. Soc. London. Ser. B.* 196, 251–265.
7. Antonjuk, D. J., Birdsall, B., Burgen, A. S. V., Cheung, H. T. A., Clore, G. M., Feeney, J., Gronenborn, A., Roberts, G. C. K., and Tran, W. (1984) *Br. J. Pharmacol.* 81, 309–315.
8. Bolin, J. T., Filman, D. J., Matthews, D. A., Hamlin, R. C., and Kraut, J. (1982) *J. Biol. Chem.* 257, 13650–13662.
9. Morgan, W. D., Birdsall, B., Polshakov, V. I., Sali, D., Kompis, I., and Feeney, J. (1995) *Biochemistry* 34, 11690–11702.
10. Glushka, J., Barany, F., and Cowburn, D. (1989) *Biochem. Biophys. Res. Commun.* 164, 88–93.
11. Pascal, S. M., Yamazaki, T., Singer, A. U., Kay, L. E., and Forman-Kay, J. D. (1995) *Biochemistry* 34, 11353–11362.
12. Yamazaki, T., Pascal, S. M., Singer, A. U., Forman-Kay, J. D., and Kay, L. E. (1995) *J. Am. Chem. Soc.* 117, 3556–3564.
13. Feng, M.-H., Philippopoulos, M., MacKerell, A. D., Jr., and Lim, C. (1996) *J. Am. Chem. Soc.* 118, 11265–11277.
14. Gargaro, A. R., Frenkiel, T. A., Nieto, P. M., Birdsall, B., Polshakov, V. I., Morgan, W. D., and Feeney, J. (1996) *Eur. J. Biochem.* 238, 435–439.
15. Nieto, P. M., Birdsall, B., Morgan, W. D., Frenkiel, T. A., Gargaro, A. R., and Feeney, J. (1997) *FEBS Lett.* 405, 16–20.
16. Gargaro, A. R., Soteriou, A., Frenkiel, T. A., Bauer, C. J., Birdsall, B., Polshakov, V. I., Barsukov, I. L., Roberts, G. C. K., and Feeney, J. (1998) *J. Mol. Biol.* 277, 119–134.
17. Andrews, J., Clore, G. M., Davies, R. W., Gronenborn, A. M., Gronenborn, B., Kalderon, D., Papadopoulos, P. C., Schafer, S., Sims, P. F. G., and Stancombe, R. (1985) *Gene* 35, 217–222.
18. Dann, J. G., Ostler, G., Bjur, R. A., King, R. W., Scudder, P., Turner, P. C., Roberts, G. C. K., Burgen, A. S. V., and Harding, N. G. L. (1976) *Biochem. J.* 157, 559–571.
19. Sklenar, V., Piotto, M., Leppik, R., and Sauder, V. (1993) *J. Magn. Reson.* 102, 241–245 (Series A).

20. Shaka, A. J., Barker, P. B., and Freeman, R. (1985) *J. Magn. Reson.* 64, 547–552.
21. States, D. J., Haberkorn, R. A., and Ruben, D. J. (1982) *J. Magn. Reson.* 48, 286–292.
22. Mori, S., Abeygunawardana, O'Neil Johnson, M., and Van Zijl, P. C. M. (1995) *J. Magn. Reson.* 108, 94–98 (Series B).
23. Wagner, G., Bodenhausen, G., Muller, N., Rance, M., Sorensen, O. W., Ernst, R. R., and Wüthrich, K. (1985) *J. Am. Chem. Soc.* 107, 6440–6446.
24. Wider, G., Neri, D., and Wüthrich, K. (1991) *J. Biomol. NMR* 1, 93–98.
25. Sandstrom, J., (1982) *Dynamic NMR Spectroscopy*, Academic Press, London.
26. Lancelot, G., Mayer, R., and Helene, C. (1979) *J. Am. Chem. Soc.* 101, 1569–1576.
27. Mitchell, J. B. O., Thornton, J. M., Singh, J., and Price, S. L. (1992) *J. Mol. Biol.* 226, 251–262.
28. Martorell, G., Gradwell, M. J., Birdsall, B., Bauer, C. J., Frenkiel, T. A., Cheung, H. T. A., Polshakov, V. I., Kuyper, L., and Feeney, J. (1994) *Biochemistry* 33, 12416–12426.
29. Cayley, J., Albrand, J. P., Feeney, J., Roberts, G. C. K., Piper, E. A., and Burgen, A. S. V. (1979) *Biochemistry* 18, 3886–3895.
30. Sternberg, U., and Brunner, E. (1994) *J. Magn. Reson. A* 108, 142–150.
31. Polshakov, V. I., Birdsall, B., Frenkiel, T. A., Gargaro, A. R., and Feeney, J. *Protein Sci.* In press.

BI982359U